SPACE SCIENCES

New clues to ancient water on Itokawa

Ziliang Jin* and Maitrayee Bose

We performed the first measurements of hydrogen isotopic composition and water content in nominally anhydrous minerals collected by the Hayabusa mission from the S-type asteroid Itokawa. The hydrogen isotopic composition (δD) of the measured pyroxene grains is −79 to −53‰, which is indistinguishable from that in chondritic meteorites, achondrites, and terrestrial rocks. Itokawa minerals contain water contents of 698 to 988 parts per million (ppm) weight, after correcting for water loss during parent body processes and impact events that elevated the temperature of the parent body. We infer that the Bulk Silicate Itokawa parent body originally had 160 to 510 ppm water. Asteroids like Itokawa that formed interior to the snow line could therefore have been a potential source of water (up to 0.5 Earth's oceans) during the formation of Earth and other terrestrial planets.

INTRODUCTION

Water is critical to the formation of terrestrial planets (*1*) and predicted to be essential for carbon-based life (*2*). Earth is characterized by high water abundances in its crust [15,000 to 20,000 parts per million (ppm)] and mantle (380 to 2560 ppm) (*3*). A lake of liquid water was recently detected beneath the frozen ice cap at Mars' south pole (*4*). The Moon and Vestoids also contain magmatic water, as has been shown in recent studies (*5*, *6*). The origin of water in the inner solar system bodies is constantly debated (*5*–*7*). According to the Grand Tack model, volatile-rich asteroids were scattered into the inner confines, within 10 million years (Ma) after the formation of refractory inclusions, and supplied water to the terrestrial planets as they were growing (*7*). The late accretion theory suggests that additional water was delivered late (tens of million years after Jupiter formed) in the solar system history by impacts of water-rich asteroids and/or comets from the outer solar system (*8*). Alternative scenarios that can explain Earth's water sources include accretion of ice in pebble-sized bodies as the snow line migrated (*9*) and ingassing of molecular hydrogen by growing planets (*10*). Thus, there are large uncertainties in the timing, source regions, and amount of water delivered to terrestrial planets.

Investigating whether the early building materials or planetesimals contain abundant water can aid in our understanding of the origin of water in terrestrial planets, especially Earth. S-type asteroids are one of the most common objects in the asteroid belt and originally formed at a heliocentric distance of 0.3 to 3 astronomical units (AU) (*7*). These asteroids are generally small (≤20 km) and did not contain adequate amounts of ^{26}Al when they formed and so escaped differentiation (*11*). Therefore, S-type asteroids should have recorded and possibly retained information about primordial nebular water. Fortuitously, in 2010, the Japan Aerospace Exploration Agency's (JAXA) sample return mission Hayabusa to the S-type asteroid Itokawa 25143 collected and returned more than 1500 particles from the Muses Sea (*12*). Here, we present the deuterium-to-hydrogen (D/H) isotopic ratios and water abundance in the silicate minerals from Itokawa regolith and evaluate the effects of secondary processes, such as space weathering, thermal metamorphism, and impacts to Itokawa's water inventory. Our findings suggest that nominally anhydrous minerals (NAMs), e.g., pyroxenes from Itokawa, are water rich. The D/H ratios of the NAMs in Itokawa particles are akin to standard mean ocean water (SMOW), and we discuss the implications to the origin of water on Earth.

School of Earth and Space Exploration, Arizona State University, Tempe, AZ 85287-1404, USA.
*Corresponding author. Email: ziliang.jin@asu.edu

RESULTS

In the returned samples from Itokawa, olivine and pyroxene are the dominant phases (up to 80 volume %) (*12*). These refractory phases must have condensed from a cooling gas of solar composition when the condensates were in equilibrium with the vapor (*13*). We measured in situ water contents and D/H ratios of two low-calcium orthopyroxene (LPx) grains from Hayabusa particles RA-QD02-0057 and RA-QD02-0061 using a nanoscale secondary ion mass spectrometry (NanoSIMS) 50L. RA-QD02-0057 LPx grain has a water content of 970 ± 93 ppm weight (2σ), while RA-QD02-0061 LPx grain contains 680 ± 65 ppm (2σ) water. The δD values of the grains from RA-QD02-0057 and RA-QD02-0061 normalized to SMOW (D/H = 1.5576×10^{-4}) are −68 ± 70‰ (2σ) and −42 ± 69‰ (2σ), respectively. In addition to the Itokawa particles, the D/H ratios of several pyroxenes from an LL6 ordinary chondrite, Larkman Nunatak LAR 12036, were measured to compare to Itokawa minerals. LAR 12036, a pristine Antarctic meteorite, was chosen for this comparison because Itokawa belongs to the LL class of ordinary chondrites with petrologic types 4 to 6 (*14*). The δD_{SMOW} values of these pyroxenes range from −241 ± 19‰ to 12 ± 23‰ (2σ) with a median value of −33 ± 92‰ [2 standard errors of the median (2 SM)]. The measured pyroxenes have water contents ranging from 565 to 1303 ppm with a median water content of 801 ± 335 ppm (2 SM).

DISCUSSION

Several processes could have modified the content and the hydrogen isotope ratio of the original water that was incorporated into the Itokawa pyroxenes during condensation. Therefore, we made corrections to infer the primordial Itokawa hydrogen isotope composition and content. The solar wind (SW) bearing low-energy particles (~1 keV) contains abundant protons (H^+) and $^4He^{2+}$ ions (*15*). In addition, highly energetic (>1 GeV) galactic cosmic rays (GCRs) mostly composed of H^+ and heavier nuclides stream from outside the solar system (*16*). Implantation and spallation nuclear reactions induced by SW and GCRs continuously produce H and D into the Itokawa regolith over the history of the solar system, which can enhance the H/O ratio or water content and alter the D/H ratio. Although the structurally disordered rims (50 to 100 nm) in Itokawa grains were most likely produced by SW implantation

(*17*), the SW contribution to the water contents measured in the interior of the pyroxene grains is negligible. We calculated the cosmogenic contribution based on the reported H and D production rates (*18*, *19*) and a short exposure age of 8 Ma of Itokawa regolith (*20*). A fairly small amount of water, <1 ppm, was produced by GCR spallation in the Itokawa particles, and the δD_{SMOW} values of the measured grains increase by ~1‰ (Supplementary Text).

Itokawa was originally larger than 20 km in radius and was disrupted by a catastrophic impact. Some fragments and boulders re-accreted into the present rubble-pile asteroid (*12*). Before its disruption, the parent body of asteroid Itokawa was heated to temperatures of ~600° to 800°C during the process of thermal metamorphism (*12*), but these temperatures were not high enough to initiate melting. Heating during thermal metamorphism can cause diffusive loss of interstitial hydrogen and result in dehydration of minerals. This process, in addition to small temperature enhancements in the history of Itokawa, would have resulted in the melting of ice and release of fluids, which have implications for the aqueous activity on S-type asteroids, such as the formation of apatite and occurrence of bleached chondrules (*21*). Apatite in ordinary chondrites is generally considered as a secondary phase that possibly formed via an interface-coupled dissolution-reprecipitation mechanism during metasomatism, where aqueous fluids played a substantial role in the ordinary chondrite parent bodies (*21*). A small proportion (<1%) of apatite has been identified in the returned particles (*12*). Our results prove that water is present in sufficient quantities within pyroxene minerals, and release of these volatiles during thermal metamorphism can be the source of the initial fluids required for the closed-system reactions to occur.

To evaluate diffusive volatile loss from the Itokawa parent body during thermal metamorphism, we developed a thermal diffusion model, using the one-dimensional solution to Fick's second law of diffusion [(*22*) and Supplementary Text], and applied specific boundary conditions with the knowledge of Itokawa's geologic history. The starting water contents are identical in all our simulations. The peak metamorphic temperature of 800°C was used in the thermal modeling of Itokawa parent body, which constrained the size of the parent body to be between 20 and 30 km (*23*). We assumed a spherical parent body of Itokawa (25 km in radius) in our diffusion model. The porosity of the parent body in our simulations was set to 25% because the pressure due to impacts can produce post-shock temperatures of 900°C in materials with a porosity of ~20 to 30% (*24*). We also assumed that the maximum duration of thermal metamorphism was 10 Ma because heating of small undifferentiated bodies is suggested to occur in the first 10 Ma of the solar system evolution (*25*). Last, to quantify the amount of water that is lost, the simulations assumed that the measured grains (from RA-QD02-0057 and RA-QD02-0061) were buried at three different depths, viz., 100 m, 1 km, and 10 km, from the asteroid surface, when the bodies were heated internally. Our diffusion model shows that, at a depth of 100 m from the asteroid surface, dehydration can reduce the water content in the pyroxene grains by 213 ppm at a temperature of 800°C (Fig. 1A), whereas the amount of water loss is <15 ppm, if the temperature was 600°C (Fig. 1A). On the other hand, at a depth of 1 km (Fig. 1B) or greater (10 km; Fig. 1C) and at a temperature of 800°C, water loss is limited to <25 ppm.

In addition to dehydration by thermal metamorphism, collisions can cause considerable localized heating and lead to loss of volatiles (*26*). The parent body of Itokawa has been argued to have experienced multiple shock events, as indicated by the olivines that show evidence of moderate shock features, such as dislocations and local variations in the

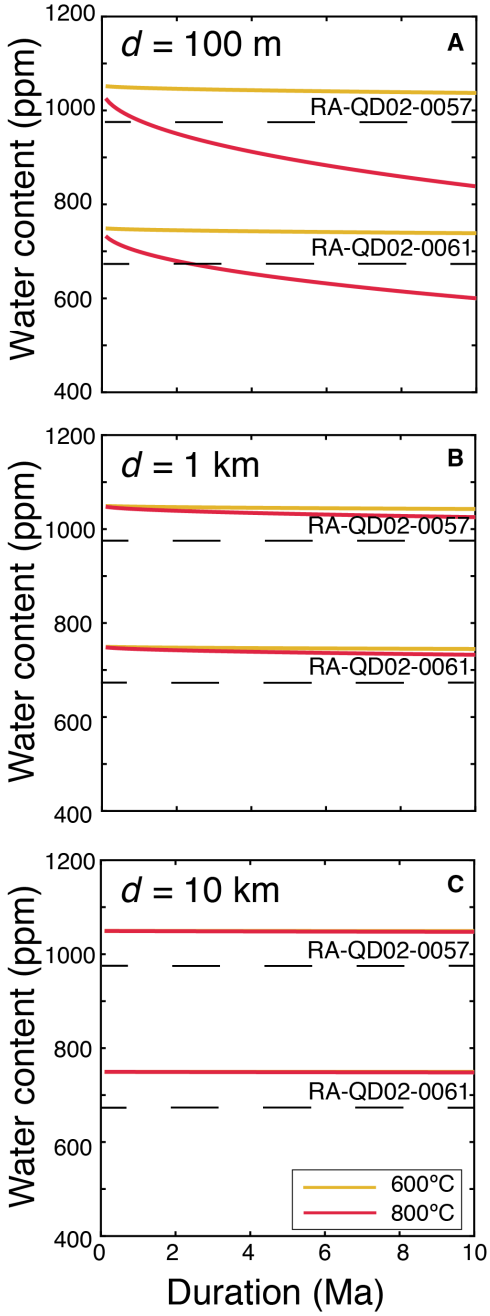

Fig. 1. Thermal diffusion model to quantify water loss during thermal metamorphism at temperatures of 600° to 800°C. The model is based on the analytical solution to the diffusion equation discussed by Ingrin and Blanchard (*22*). A sphere 25 km in radius with pyroxene composition was heated to temperatures of 600° and 800°C for a duration of 10 Ma. The water contents in pyroxene grains at distances of 100 m (**A**), 1 km (**B**), and 10 km (**C**) from the top surface of the sphere are plotted against the duration of thermal metamorphism. Dashed lines indicate the measured concentrations of water in two Itokawa grains. Higher temperatures and shallower depths result in larger diffusivity and enhanced loss of water. At a distance of 100 m, heating at 800°C would result in a loss of up to ~213 ppm water. When the distance from the surface is larger than 1 km, water loss is less than 25 ppm.

degree of silicate crystallinity (*12*). A model based on $^{40}Ar/^{39}Ar$ analyses of Itokawa olivine suggests that Itokawa parent body experienced a post-shock temperature of 900°C during an impact event (*24*). The post-shock temperature of L-chondritic parent body could have reached 1500°C and resulted in melting of minerals (*27*). Evidence of crystallization from a partial melt was speculated when remote near-infrared observations during Hayabusa flybys reported Fe-rich pyroxene compositions of Itokawa surface compared to ordinary chondrites (*28*). However, closeup images of Itokawa LPx grains do not show melt features, and Fe-rich nanoparticles were identified on olivine surfaces (*29*). Therefore, the post-shock temperature was most likely lower than the crystallization temperature of pyroxene, which is ~1200°C (*30*). Furthermore, the rapid cooling rates [200° to 600°C/thousand years (ka)] estimated for several H, L, and LL ordinary chondrites indicate a short duration of the post-shock temperatures (*31*). Accordingly, we simulated the loss of water using our thermal diffusion model at temperatures of 800°, 1000°, and 1200°C and with a short annealing time of 2 ka. As shown in Fig. 2A, when the post-shock temperature reaches 1200°C, the water loss is as high as ~80 ppm at a depth close to the surface (100 m); lower temperatures (<1000°C) cause less water loss (<21 ppm). Because of the short annealing time, the water loss of deeper buried grains (1 and 10 km) is limited (<8 ppm) even at the highest temperatures (Fig. 2, B and C).

We know that the equilibrated Itokawa particles were located at considerable depths within the Itokawa parent body during thermal metamorphism (*12*) and possibly also during impacts. However, the specific locations of the LPx grains of RA-QD02-0057 and RA-QD02-0061, when they experienced the high-temperature events, are unknown. Thus, we mathematically estimated the amount of water that would be lost from the grains, if they were located under different depths. We divided the Itokawa parent body (25 km in radius) into 250 concentric onion-like layers, and each layer (n) was assumed to be 100 m thick. The average amount of water (E[X]) lost at a distinct temperature is given by the equation

$$\mathrm{E}[X] = \sum_{n=1}^{250} p_n \, x_n \qquad (1)$$

where p_n is the probability of the LPx grain to occur at a distance of n·100 m from the top surface and x_n is the corresponding amount of water lost at this depth based on our thermal diffusion model (Supplementary Text). On the basis of Eq. 1, we calculated that the average amount of water lost from the LPx grain caused by the 10-Ma thermal metamorphism at 800°C is ~12 ppm. Furthermore, the highest post-shock temperature (1200°C) triggered by the impact event will result in ~5 ppm water during the 2-ka period. Taking the water lost by both these mechanisms into account, we report that the primordial water concentrations of two Itokawa grains are 988 ± 93 ppm (2σ) and 698 ± 65 ppm (2σ).

The D/H ratio can be used as a probe to constrain the nebular composition at the time of Itokawa's formation and Itokawa's role in the existence of water on Earth. Dehydration experiments have revealed the diffusion-driven D/H fractionation in garnet (*32*). Thus, fractionation of hydrogen isotopes in Itokawa LPx grains needs to be evaluated. The isotopic fractionation is indicated by the Rayleigh distillation equation (*32*)

$$\delta\mathrm{D}‰ = 1000 \times \left(F^{\left(\frac{1}{\alpha}-1\right)} - 1\right) \qquad (2)$$

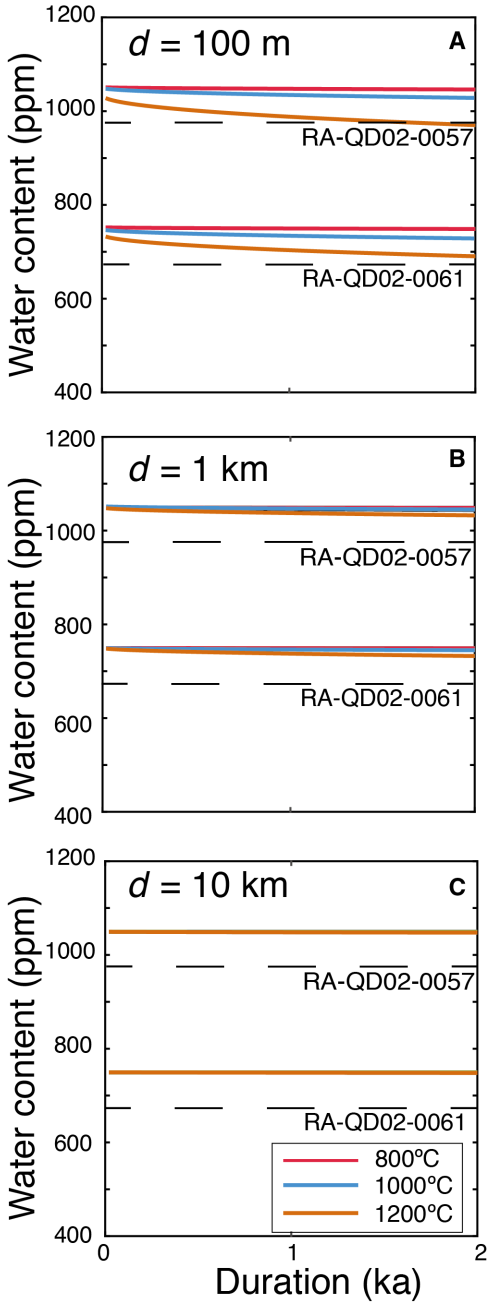

Fig. 2. Modeling of dehydration due to an impact event. It shows the residual water contents in pyroxene grains at distances of 100 m (**A**), 1 km (**B**), and 10 km (**C**) from the surface of a sphere with a radius of 25 km. The same diffusion model has been used as in Fig. 1, although different input parameters, e.g., post-shock temperatures (800°, 1000°, and 1200°C) and cooling duration (2 ka), are subjected to the sphere. Dashed lines indicate the measured concentrations of water in two Itokawa grains. When temperature is lower than 1000°C, the loss of water is limited to be <25 ppm for all cases. The highest post-shock temperature (1200°C) causes ~80 ppm loss of water at a distance of 100 m. The loss of water is insignificant if the pyroxene occurs at a distance that is larger than 1 km from the surface.

where F is the fraction of hydrogen in the solid residue and α is the fractionation factor. On the basis of our water diffusion model, the water remaining in the pyroxene accounts for a fraction of 97% (F = 0.97). Using an α value of 1.414 for an ideal gas (*32*), we calculated that the

δD values of Itokawa pyroxenes are enhanced by ~10‰. After taking the dehydration processes and GCR spallation into consideration, the original δD_{SMOW} value of Itokawa LPx grain RA-QD02-0057 is −79 ± 70‰ and that for grain RA-QD02-0061 is −53 ± 69‰. Itokawa is compatible with an LL4 to LL6 chondrite classification (*14*), and therefore, the proportion of the matrix, bearing deuterium-rich insoluble organic matter, compared to NAMs would be fairly low (*33*). Accordingly, the D/H ratio of Itokawa is essentially represented by those of the NAMs (Supplementary Text). The δD_{SMOW} of Itokawa is indistinguishable from those of apatite and melt inclusions from lunar and martian samples, bulk carbonaceous chondrites, and apatite from Vesta (Fig. 3). In addition, the δD_{SMOW} values of pyroxenes in Itokawa, LAR 12036 (median value = −33 ± 92‰, 2 SM), and Bishunpur [median value = −52 ± 68‰, 2 SM (*34*)] are the same within analytical uncertainties (Fig. 4), implying that S-type asteroid bodies probably accreted water from the same region in the proto-solar nebula and by similar processes. The heterogeneity observed in the pyroxenes from LAR 12036 and Bishunpur possibly reflects the D-rich water composition that has experienced variable degrees of isotopic exchange or may reflect various degrees of degassing. The δD_{SMOW} value of Itokawa lies in the δD range of terrestrial samples and indicates a common source of water for Earth and S-type asteroid bodies.

The water contents of Itokawa LPx grains (698 to 988 ppm) are the same within errors compared to those in pyroxenes from LAR 12036 (median value = 801 ± 335 ppm) and Bishunpur chondrules (median value = 1090 ± 359 ppm; Fig. 5) (*34*). Itokawa contains 67.2 weight % (wt %) olivine, 18.1 wt % LPx, and 2.6 wt % high-calcium pyroxene (HPx) (*12*). The large proportion of olivines and pyroxenes in Itokawa and possibly other S-type asteroids makes them dominant components in controlling the volatile composition of planetesimals or planetary embryos that formed out of these minerals. On the basis of the known mineral proportions (*12*) and using assumptions from experiments on terrestrial NAMs, we computed Itokawa's bulk water content. The first assumption is that HPx can accommodate twice the amount of water compared to LPx in terrestrial rocks under equilibrium conditions (*3*). Second, the amount of water that is incorporated in olivine is generally 10 to 25 times less than that in orthopyroxene under 0.5 to 4 GPa and 1000° to 1380°C conditions (*35*). Third, the only reported water content in olivine from Bishunpur ordinary chondrite has a range of 76 to 399 ppm (*34*), and we assume that Itokawa olivine has the same concentration of water as Bishunpur. On the basis of these assumptions, we estimated the water content of bulk silicate Itokawa (BSI) to be 160 to 510 ppm, which is the first bulk water estimate for an S-type asteroid. The estimated water content of BSI is relatively higher than those in bulk silicate Moon [133 to 292 ppm (*5*)], martian mantle [73 to 290 ppm (*36*)], and two large near-Earth S-type asteroids 433 Eros and 1036 Ganymed with water concentrations of ~30 to 300 ppm (*37*), which are considered as lower limits (Supplementary Text).

The high water abundance of Itokawa, as presented here, and previously reported signatures of aqueous activity that occur in ordinary

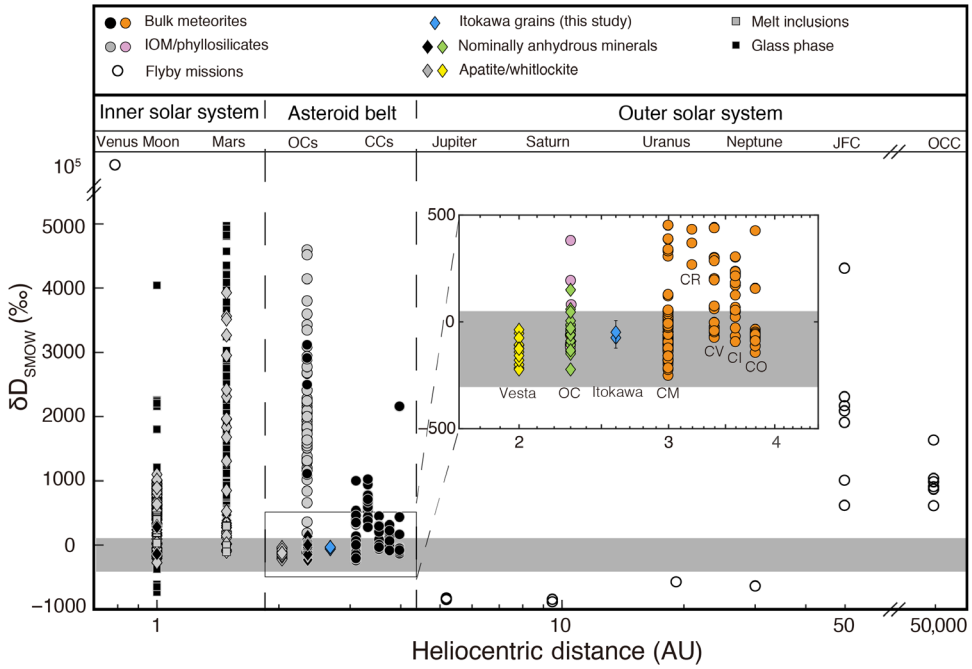

Fig. 3. Hydrogen isotope compositions of objects in the solar system expressed as δD_{SMOW}. Itokawa LPx grains (−79 ± 70‰ for RA-QD02-0057 and −53 ± 69‰ for RA-QD02-0061) are shown in blue diamonds. Except for Itokawa grains, no errors have been plotted for clarity. The gray shaded region represents the range of terrestrial samples. Jupiter family comets (JFCs) are in the Kuiper Belt that extends from 30 to 50 AU; Oort cloud comets (OCCs) occupy a vast space from 2000 to 50,000 AU from the Sun. We have plotted all Jupiter family comets and Oort cloud comets at 50 and 50,000 AU, respectively, instead of their current locations. The measured phases from OCs are separated into D-rich matrices, D-rich bulk rock, and low-δD NAMs. The high δD_{SMOW} values for the martian glass phases and apatite likely reflect interaction with the D-rich martian atmosphere and are not relevant while determining the bulk mantle water on Mars. The inset shows the δD_{SMOW} of samples from the asteroid belt, such as eucrites, ordinary chondrites (OCs), and carbonaceous chondrite (CCs). Our measurements show that the δD_{SMOW} values of two Itokawa grains, apatite from Vesta, most NAMs from OCs, and some of the bulk carbonaceous chondrites fall within the range of terrestrial samples. IOM, insoluble organic matter (see Supplementary Text for data and references).

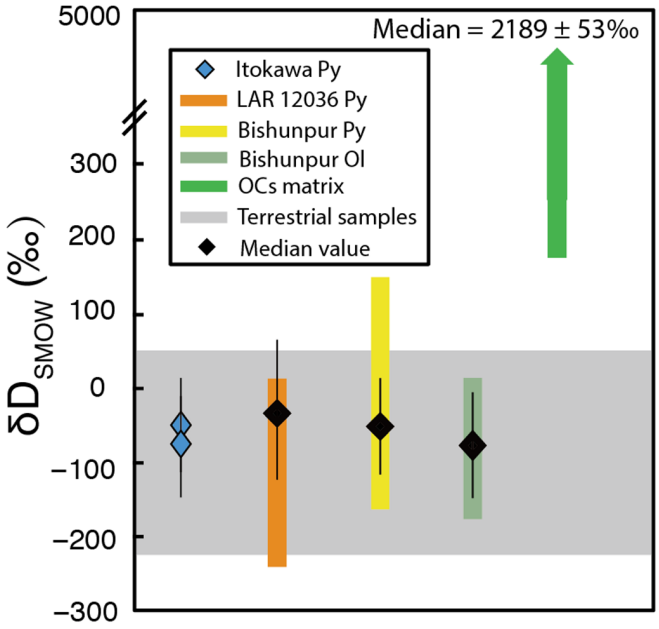

Fig. 4. δD_{SMOW} (‰) of pyroxene and olivine from LAR 12036 and Bishunpur, and matrices from ordinary chondrites. The black diamonds indicate the median δD_{SMOW} of NAMs from ordinary chondrites. The errors are 2 SM. The δD_{SMOW} values of pyroxene and olivine from ordinary chondrites fall in a range of −250 to +150‰. The median δD_{SMOW} values of NAMs from ordinary chondrites are within a range of −100 to 0‰ and fall in the range of terrestrial samples, which is indicated by the gray shaded area. The δD_{SMOW} values of phases in the matrices of ordinary chondrite have a range of +171 to +4562‰, which are higher than that of NAMs from ordinary chondrites and terrestrial samples (see Supplementary Text for data). Py, pyroxene; Ol, olivine.

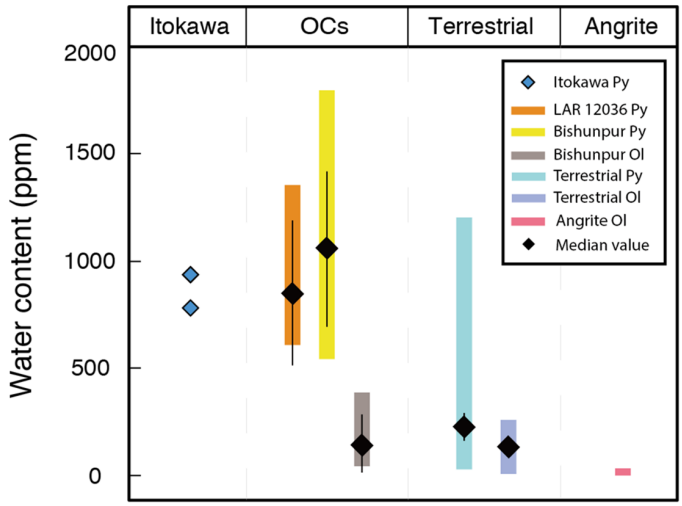

Fig. 5. Water contents (ppm) of two measured Itokawa grains and the concentrations of water in pyroxene and olivine from LL6 LAR 12036, LL3.1 Bishunpur ordinary chondrite, terrestrial rocks, and angrite. The black diamonds indicate the median water contents of NAMs in each group. The errors are 2 SM, and some errors are smaller than the size of the symbols. Pyroxenes from Itokawa, LAR 12036, and Bishunpur ordinary chondrites have comparable water contents, and their median water contents are higher than those of terrestrial pyroxenes. The olivines from ordinary chondrites and terrestrial samples have low water contents. The angrite samples are drier (see Supplementary Text for data).

chondrite parent bodies prove that S-type asteroids formed in the inner solar system were hydrous despite high temperatures and could have been a potential source for Earth's water. On the basis of our data, we propose an alternative scenario for the origin of water on Earth: Early in the solar system history, a fraction of hydrogen was incorporated into the NAMs by adsorption and associated hydroxylation, which could occur at high temperatures (up to ~1200°C) and nebular pressures (*38*). These water-bearing refractory NAMs grew by mutual sticking into millimeter- to centimeter-sized, chemically diverse pebbles by gas drag in the dense protoplanetary disk (*39*). Subsequently, streaming instabilities concentrated these aggregates by pebble accretion and led to the formation of planetesimals like Itokawa (*39*). The continual growth of the planetesimals into planetary embryos and the growth of planetary embryos into planets occurred (*40*). Thus, the condensation of the hydrous NAMs and the production of millimeter- to centimeter-sized aggregates from these precursor minerals may be a key process promoting the incorporation of water in rocky planets, especially Earth. We estimated the amount of water that could be delivered to proto-Earth by this process using (*41*). In this work, an assortment of materials from ordinary, enstatite, and carbonaceous chondrites was modeled to accrete and form Earth during several, separate stages of planetary growth, and the constraints imposed were high-precision isotopic data (lithophile elements O, Ca, Ti, and Nd; moderately siderophile elements Cr, Ni, and Mo; and a highly siderophile element, Ru). In the first stage, 40% of the accreting materials was proposed to be ordinary chondrites (*41*), which indicates that S-type asteroids, like Itokawa, could have delivered about 0.5 oceans of water to Earth (1 Earth's ocean = 1.4×10^{21} kg; Supplementary Text).

During accretion, localized irradiation processes within 3 AU could not have modified the primitive hydrogen signatures of the NAMs (*42*). Therefore, the accreted pebbles from the NAMs and planetesimals would preserve the D/H ratio acquired during formation in agreement with our observations: Itokawa, Earth, and parent bodies of LAR 12036 and Bishunpur ordinary chondrites, all formed in the inner solar system and exhibit comparable D/H ratios. The other process that could change the primordial D/H ratios acquired in the nebula is differentiation. However, the contributions from the coupled ingassing and degassing of volatiles during differentiation are poorly understood and have not been accurately quantified. The reported most negative δD value of melt inclusion from Baffin Island picrites (δD_{SMOW} = −218‰) represents the primordial water in Earth's deep mantle (*43*). Accordingly, we use a range of δD for Earth (−218 to +46‰) in this study, despite the possible yet unknown degree of modification during differentiation.

Minerals from the Muses Sea on Itokawa show evidence of water that was not lost despite their thermal history and micrometeoroid impacts and have hydrogen isotopic compositions that are indistinguishable from Earth. The hydration of Earth could have occurred during its accretion phase when it directly inherited nebular water incorporated into NAMs, followed by the collisions of S-type asteroids. S-type planetesimals and parent bodies of ordinary chondrites are likely a critical source of water and several other elements for the terrestrial planets. These inferences were possible only because of in situ isotopic measurements on returned samples of asteroid regolith. The Hayabusa mission has expanded our knowledge of the volatile contents of planetesimals that have played an influential role in the process of Earth's formation. A similar mechanism of water production may be ubiquitous in rocky exoplanets.

MATERIALS AND METHODS

Sample descriptions

We were allocated five particles from JAXA, of which two contain large domains that had confirmed LPx mineralogy. In this study, we define RA-QD02-0057 and RA-QD02-0061 as "particles." Minerals within each particle are referred to as "grains" or "mineral grains." Grain RA-QD02-0057 is one single-phase LPx grain (fig. S1) with a size of ~20 μm by 40 μm. RA-QD02-0061 is ~30 μm by 45 μm in size and composed of multiple mineral grains, including LPx, plagioclase, troilite, and taenite (fig. S1). The troilite and taenite are micrometer-sized subgrains within the multimineralic particle. In the study by Yurimoto *et al.* (*14*), oxygen isotope measurements on the LPx grains show that these grains are depleted in ^{16}O relative to terrestrial minerals. The $\Delta^{17}O$ values with respect to SMOW for RA-QD02-0057 and RA-QD02-0061 are 1.16 and 1.47‰, respectively. The $\delta^{18}O$ values are 5.1‰ for RA-QD02-0057 and 3.7‰ for RA-QD02-0061 (fig. S2). On the basis of the oxygen isotopic measurements on pyroxene, olivine, and plagioclase minerals from Itokawa, it has been suggested that the composition of the Itokawa asteroid is equivalent to types 4 to 6 in the L or LL chondrite group; Itokawa-like asteroids are the sources of equilibrated ordinary chondrites (*14*).

For comparison, we measured the water content and hydrogen isotope of pyroxenes from the LL6 Larkman Nunatak 12036 (LAR 12036) ordinary chondrite. The dominant mineral phases in LAR 12036 are olivine and LPx (fig. S1).

Mounting of samples and standards

When the samples arrived at Arizona State University, they were sealed in aluminum envelopes that were purged in nitrogen. The previously analyzed Itokawa grains were embedded in epoxy into 6-mm stubs, polished flat, and coated with a conductive gold coat required for SIMS analyses (fig. S1). We did not want to risk losing the particles or fracturing the particles along grain boundaries during sample preparation (e.g., removal of particles from epoxy, polishing, and mounting in indium); hence, we directly pressed the epoxy discs into high-purity (99.9%) indium. The mounting procedures were conducted in a Class 10,000 clean lab under clean benches with <100 particles/cm^3. The mounting of the standards took ~8 hours, during which we followed a strict protocol where no water was used during polishing and mounting. The standards were first mounted in epoxy (EpoxiCure 2, the mass ratio of hardener/resin = 23/100), polished by a 0.5-μm diamond film (Vender: Struers), removed from the epoxy after 24-hour steeping in 100% acetone, and pressed into indium. All mounted samples were coated with conductive gold layers (35 nm) and kept in a 50°C oven for 24 hours. Then, the samples for NanoSIMS measurements were placed in the ultrahigh vacuum chambers of the NanoSIMS for 10 days before the measurements.

We used four terrestrial samples, namely, 116610-18, KH03-04, KH03-27, and ALV-519, as standards for the NanoSIMS measurement of H_2O contents and D/H ratios. 116610-18 and KH03-04 are orthopyroxenes with water contents of 119 ± 22 ppm (2σ) and 216 ± 28 ppm (2σ), respectively (*43*). The sample KH03-27 is the clinopyroxene and has a water content of 367 ± 98 ppm (2σ) (*43*). ALV-519 is a piece of basaltic glass and contains 1700 ± 86 ppm (2σ) water (*44*). All the reference standards and two Itokawa grains were placed in one sample holder (fig. S1).

A polished thin section of LAR 12036 allocated from NASA was measured in the IMS 6f. The references for IMS 6f measurements were 116610-18, PMR-53, and ALV-519. The PMR-53 (268 ± 16 ppm H_2O, 2σ) is a terrestrial clinopyroxene megacryst found in kimberlite (*45*). All three references were prepared and mounted following the same procedures as those for NanoSIMS measurements.

NanoSIMS analysis

D/H ratios and H_2O concentrations of the standards and Itokawa particles were measured by the Cameca Ametek NanoSIMS 50L at Arizona State University. A 16-keV Cs^+ primary beam of ~250 pA (D1-5 aperture, 100 μm diameter) was rastered on a 5-μm by 5-μm surface on the grain. The size of the primary beam was ~3 μm in diameter. H^-, D^-, $^{12}C^-$, and $^{18}O^-$ were measured simultaneously with no entrance slit and aperture slit. The Cameca mass resolution for the spectrometer was ~1300. All measurements were performed in isotope mode. The counting time was set to 1 ms/pixel; the measurements on the standards and samples consisted of 240 to 480 cycles. The secondary ion signal from the internal 25% of the rastered area was collected using electronic gating. The electron gun (~1100 nA) was used to compensate for the charging of the sample surface. Before the data collection, the sample surface was presputtered with a raster of 10 μm by 10 μm for ~15 min to implant cesium and to remove surface contamination. The $^{12}C^-$ intensity was primarily used to monitor the contribution from epoxy, which contains high concentrations of hydrogen and carbon. Before measurements were conducted, we monitored the $^{12}C^-$ signal to ensure that it was low and stable (fig. S3). This was particularly important to ensure that the beam was not hitting cracks on the grain surfaces.

Before the measurements, the analysis chamber was baked for 5 hours to achieve a good vacuum. In addition, the Ti sublimation ion pump was used for the analysis chamber, which significantly reduced the background hydrogen. The pressure of the analysis chamber was constant under conditions of (2 to 3) × 10^{-10} torr, as shown in fig. S3. During the measurements, the background was monitored under the "beam-off" mode (when electron beam was on and Cs^+ beam was off) for 20 cycles before and after the measurements ("beam-on" mode). We recorded the count rates of hydrogen and deuterium and subtracted them from those obtained in beam-on mode. We used the corrected count rates of hydrogen and deuterium to calculate the isotopic ratios, such as D^-/H^- and $H^-/^{18}O^-$, which are then used for estimation of the water contents and δD values.

Cameca IMS 6f analyses

The measurements of D/H ratios in the pyroxenes from LAR 12036 ordinary chondrite were performed on the Cameca IMS 6f at Arizona State University. We used a 10- to 13-nA Cs^+ ion beam with a beam diameter of approximately 25 μm. The Cs^+ primary beam, with an impact energy of 15 keV, was rastered on a 35-μm by 35-μm surface area. The area of interest was sputtered for 120 s before the analysis to remove the gold film, reduce any surface contamination, and establish steady-state sputtering conditions. A normal incidence electron gun was used to compensate for the sample surface charge during the measurements. The field aperture set the analyzed area to 15 μm diameter, which reduced background associated with crater edge effects. The mass spectrometer was operated with a mass resolution of ~800. Each measurement was composed of 50 cycles of measuring H^- and D^- on an electron multiplier, with counting times of 1 and 10 s, respectively. At the end of each measurement, $^{16}O^-$ was measured using a Faraday cup/electrometer. The vacuum in the analytical chamber was ~3 × 10^{-9} torr during the analyses.

After the measurements, reflected light images were acquired to check for location of cracks and identify the non-flat topography of

the craters. We choose only the good data points that show the absence of cracks or mixture of phases, a flat-bottomed crater, and "ideal" flat hydrogen and D/H signals, as shown in fig. S4.

SUPPLEMENTARY MATERIALS

Supplementary material for this article is available at http://advances.sciencemag.org/cgi/content/full/5/5/eaav8106/DC1

Supplementary Text

Fig. S1. Itokawa particles, overview of LAR 12036 ordinary chondrite, and sample holder for NanoSIMS measurements.

Fig. S2. Reported oxygen isotopic compositions of Itokawa minerals [modified after *14*].

Fig. S3. SIMS craters on Itokawa particles and ion intensities during their NanoSIMS measurements.

Fig. S4. Representative reflected-light images of the analyzed spots after Cameca IMS 6f analyses and the H^- counting rates during the analyses.

Fig. S5. Calibrations of water contents and hydrogen isotope compositions using terrestrial standards.

Fig. S6. The onion shell model of parent body used for expected water loss calculation.

Table S1. Water concentration and D/H ratios of reference standards and Itokawa grains.

Table S2. D/H ratios of reference standards and adopted pyroxene from LAR 12036 ordinary chondrite.

Table S3. Simulated water loss caused by thermal metamorphism and impact events using the thermal diffusion model.

Table S4. Estimated average water loss of the assumed 25-km-radius parent body caused by thermal metamorphism and impact events.

References (*46*–*98*)

REFERENCES AND NOTES

1. S. M. Tikoo, L. T. Elkins-Tanton, The fate of water within Earth and super-Earths and implications for plate tectonics. *Philos. Trans. A Math. Phys. Eng. Sci.* **375**, 20150394 (2017).
2. F. Westall, A. Brack, The importance of water for life. *Space Sci. Rev.* **214**, 50 (2018).
3. A. H. Peslier, M. Schönbächler, H. Busemann, S.-I. Karato, Water in the Earth's interior: Distribution and origin. *Space Sci. Rev.* **212**, 743–810 (2017).
4. R. Orosei, S. E. Lauro, E. Pettinelli, A. Cicchetti, M. Coradini, B. Cosciotti, F. Di Paolo, E. Flamini, E. Mattei, M. Pajola, F. Soldovieri, M. Cartacci, F. Cassenti, A. Frigeri, S. Giuppi, R. Martufi, A. Masdea, G. Mitri, C. Nenna, R. Noschese, M. Restano, R. Seu, Radar evidence of subglacial liquid water on Mars. *Science* **361**, 490–493 (2018).
5. E. H. Hauri, A. E. Saal, M. J. Rutherford, J. A. Van Orman, Water in the Moon's interior: Truth and consequences. *Earth Planet. Sci. Lett.* **409**, 252–264 (2015).
6. A. R. Sarafian, S. G. Nielsen, H. R. Marschall, F. M. McCubbin, B. D. Monteleone, Early accretion of water in the inner solar system from a carbonaceous chondrite-like source. *Science* **346**, 623–626 (2014).
7. K. J. Walsh, A. Morbidelli, S. N. Raymond, D. P. O'Brien, A. M. Mandell, A low mass for Mars from Jupiter's early gas-driven migration. *Nature* **475**, 206–209 (2011).
8. A. Morbidelli, J. Chambers, J. I. Lunine, J. M. Petit, F. Robert, G. B. Valsecchi, K. E. Cyr, Source regions and timescales for the delivery of water to the Earth. *Meteorit. Planet. Sci.* **35**, 1309–1320 (2000).
9. T. Sato, S. Okuzumi, S. Ida, On the water delivery to terrestrial embryos by ice pebble accretion. *Astron. Astrophys.* **589**, A15 (2016).
10. Z. D. Sharp, Nebular ingassing as a source of volatiles to the terrestrial planets. *Chem. Geol.* **448**, 137–150 (2017).
11. N. Moskovitz, E. Gaidos, Differentiation of planetesimals and the thermal consequences of melt migration. *Meteorit. Planet. Sci.* **46**, 903–918 (2011).
12. T. Nakamura, T. Noguchi, M. Tanaka, M. E. Zolensky, M. Kimura, A. Tsuchiyama, A. Nakato, T. Ogami, H. Ishida, M. Uesugi, T. Yada, K. Shirai, A. Fujimura, R. Okazaki, S. A. Sandford, Y. Ishibashi, M. Abe, T. Okada, M. Ueno, T. Mukai, M. Yoshikawa, J. Kawaguchi, Itokawa dust particles: A direct link between S-type asteroids and ordinary chondrites. *Science* **333**, 1113–1116 (2011).
13. L. Grossman, Condensation in the primitive solar nebula. *Geochim. Cosmochim. Acta* **36**, 597–619 (1972).
14. H. Yurimoto, K.-i. Abe, M. Abe, M. Ebihara, A. Fujimura, M. Hashiguchi, K. Hashizume, T. R. Ireland, S. Itoh, J. Katayama, C. Kato, Oxygen isotopic compositions of asteroidal materials returned from Itokawa by the Hayabusa mission. *Science* **333**, 1116–1119 (2011).
15. S. J. Bame, A. J. Hundhausen, J. R. Asbridge, I. B. Strong, Solar wind ion composition. *Phys. Rev. Lett.* **20**, 393–395 (1968).
16. J. A. Simpson, Elemental and isotopic composition of the galactic cosmic rays. *Annu. Rev. Nucl. Part. Sci.* **33**, 323–382 (1983).
17. L. P. Keller, E. L. Berger, A transmission electron microscope study of Itokawa regolith grains. *Earth Planets Space* **66**, 71 (2014).
18. E. Füri, E. Deloule, R. Trappitsch, The production rate of cosmogenic deuterium at the Moon's surface. *Earth Planet. Sci. Lett.* **474**, 76–82 (2017).
19. L. Merlivat, M. Lelu, G. Nief, E. Roth, Spallation deuterium in rock 70215. *Proc. Lunar Sci. Conf.* **7**, 649–658 (1976).
20. K. Nagao, R. Okazaki, T. Nakamura, Y. N. Miura, T. Osawa, K.-i. Bajo, S. Matsuda, M. Ebihara, T. R. Ireland, F. Kitajima, H. Naraoka, T. Noguchi, A. Tsuchiyama, H. Yurimoto, M. E. Zolensky, M. Uesugi, K. Shirai, M. Abe, T. Yada, Y. Ishibashi, A. Fujimura, T. Mukai, M. Ueno, T. Okada, M. Yoshikawa, J. Kawaguchi, Irradiation history of Itokawa regolith material deduced from noble gases in the Hayabusa samples. *Science* **333**, 1128–1131 (2011).
21. R. H. Jones, F. M. McCubbin, L. Dreeland, Y. Guan, P. V. Burger, C. K. Shearer, Phosphate minerals in LL chondrites: A record of the action of fluids during metamorphism on ordinary chondrite parent bodies. *Geochim. Cosmochim. Acta* **132**, 120–140 (2014).
22. J. Ingrin, M. Blanchard, Diffusion of hydrogen in minerals. *Rev. Mineral. Geochem.* **62**, 291–320 (2006).
23. S. Wakita, T. Nakamura, T. Ikeda, H. Yurimoto, Thermal modeling for a parent body of Itokawa. *Meteorit. Planet. Sci.* **49**, 228–236 (2014).
24. F. Jourdan, N. E. Timms, E. Eroglu, C. Mayers, A. Frew, P. A. Bland, G. S. Collins, T. M. Davison, M. Abe, T. Yada, Collisional history of asteroid Itokawa. *Geology* **45**, 819–822 (2017).
25. K. Keil, Thermal alteration of asteroids: Evidence from meteorites. *Planet. Space Sci.* **48**, 887–903 (2000).
26. T. M. Davison, G. S. Collins, F. J. Ciesla, Numerical modelling of heating in porous planetesimal collisions. *Icarus* **208**, 468–481 (2010).
27. Y. Li, W. Hsu, Multiple impact events on the L-chondritic parent body: Insights from SIMS U-Pb dating of Ca-phosphates in the NWA 7251 L-melt breccia. *Meteorit. Planet. Sci.* **53**, 1081–1095 (2018).
28. P. A. Abell, F. Vilas, K. S. Jarvis, M. J. Gaffey, M. S. Kelley, Mineralogical composition of (25143) Itokawa 1998 SF_{36} from visible and near-infrared reflectance spectroscopy: Evidence for partial melting. *Meteorit. Planet. Sci.* **42**, 2165–2177 (2007).
29. E. Nakamura, A. Akishima, T. Moriguti, K. Kobayashi, R. Tanaka, T. Kunihiro, T. Tsujimori, C. Sakaguchi, H. Kitagawa, T. Ota, Y. Yachi, T. Yada, M. Abe, A. Fujimura, M. Ueno, T. Mukai, M. Yoshikawa, J. Kawaguchi, Space environment of an asteroid preserved on micrograins returned by the Hayabusa spacecraft. *Proc. Natl. Acad. Sci. U.S.A.* **109**, E624–E629 (2012).
30. D. H. Lindsley, Pyroxene thermometry. *Am. Mineral.* **68**, 477–493 (1983).
31. J. Ganguly, M. Tirone, K. Domanik, Cooling rates of LL, L and H chondrites and constraints on the duration of peak thermal conditions: Diffusion kinetic modeling and implications for fragmentation of asteroids and impact resetting of petrologic types. *Geochim. Cosmochim. Acta* **192**, 135–148 (2016).
32. M. Roskosz, E. Deloule, J. Ingrin, C. Depecker, D. Laporte, S. Merkel, L. Remusat, H. Leroux, Kinetic D/H fractionation during hydration and dehydration of silicate glasses, melts and nominally anhydrous minerals. *Geochim. Cosmochim. Acta* **233**, 14–32 (2018).
33. C. M. O. Alexander, M. Fogel, H. Yabuta, G. D. Cody, The origin and evolution of chondrites recorded in the elemental and isotopic compositions of their macromolecular organic matter. *Geochim. Cosmochim. Acta* **71**, 4380–4403 (2007).
34. A. Stephant, L. Remusat, F. Robert, Water in type I chondrules of Paris CM chondrite. *Geochim. Cosmochim. Acta* **199**, 75–90 (2017).
35. E. H. Hauri, G. A. Gaetani, T. H. Green, Partitioning of water during melting of the Earth's upper mantle at H_2O-undersaturated conditions. *Earth Planet. Sci. Lett.* **248**, 715–734 (2006).
36. F. M. McCubbin, E. H. Hauri, S. M. Elardo, K. E. Vander Kaaden, J. Wang, C. K. Shearer Jr., Hydrous melting of the martian mantle produced both depleted and enriched shergottites. *Geology* **40**, 683–686 (2012).
37. A. S. Rivkin, E. S. Howell, J. P. Emery, J. Sunshine, Evidence for OH or H_2O on the surface of 433 Eros and 1036 Ganymed. *Icarus* **304**, 74–82 (2018).
38. A. Asaduzzaman, K. Muralidharan, J. Ganguly, Incorporation of water into olivine during nebular condensation: Insights from density functional theory and thermodynamics, and implications for phyllosilicate formation and terrestrial water inventory. *Meteorit. Planet. Sci.* **50**, 578–589 (2015).
39. A. Johansen, M. Lambrechts, Forming planets via pebble accretion. *Annu. Rev. Earth Planet. Sci.* **45**, 359–387 (2017).
40. S. J. Kenyon, B. C. Bromley, Terrestrial planet formation. I. The transition from oligarchic growth to chaotic growth. *Astrophys. J.* **131**, 1837–1850 (2006).
41. N. Dauphas, The isotopic nature of the Earth's accreting material through time. *Nature* **541**, 521–524 (2017).
42. M. Roskosz, B. Laurent, H. Leroux, L. Remusat, Experimental investigation of irradiation-driven hydrogen isotope fractionation in analogs of protoplanetary hydrous silicate dust. *Astrophys. J.* **832**, 55 (2016).

43. L. J. Hallis, G. R. Huss, K. Nagashima, G. J. Taylor, S. A. Halldórsson, D. R. Hilton, M. J. Mottl, K. J. Meech, Evidence for primordial water in Earth's deep mantle. *Science* **350**, 795–797 (2015).
44. K. M. Kumamoto, J. M. Warren, E. H. Hauri, New SIMS reference materials for measuring water in upper mantle minerals. *Am. Mineral.* **102**, 537–547 (2017).
45. G. R. Rossman, D. R. Bell, P. D. Ihinger, Quantitative analysis of OH in garnet and pyroxenes. *Am. Mineral.* **80**, 465–474 (1995).
46. A. Fujiwara, J. Kawaguchi, D. K. Yeomans, M. Abe, T. Mukai, T. Okada, J. Saito, H. Yano, M. Yoshikawa, D. J. Scheeres, O. Barnouin-Jha, A. F. Cheng, H. Demura, R. W. Gaskell, N. Hirata, H. Ikeda, T. Kominato, H. Miyamoto, A. M. Nakamura, R. Nakamura, S. Sasaki, K. Uesugi, The rubble-pile asteroid Itokawa as observed by Hayabusa. *Science* **312**, 1330–1334 (2006).
47. M. S. Thompson, R. Christoffersen, T. J. Zega, L. P. Keller, Microchemical and structural evidence for space weathering in soils from asteroid Itokawa. *Earth Planets Space* **66**, 89 (2014).
48. P. C. Hiemenz, R. Rajagopalan, *Principles of Colloid and Surface Chemistry* (Marcel Dekker, 1997).
49. N. Koone, Y. Shao, T. W. Zerda, Diffusion of simple liquids in porous sol–gel glass. *J. Phys. Chem.* **99**, 16976–16981 (1995).
50. D. El Abassi, A. Ibhi, B. Faiz, I. Aboudaoud, A simple method for the determination of the porosity and tortuosity of meteorites with ultrasound. *J. Geophys. Eng.* **10**, 055003 (2013).
51. R. Stalder, H. Skogby, Hydrogen diffusion in natural and synthetic orthopyroxene. *Phys. Chem. Miner.* **30**, 12–19 (2003).
52. H. Y. McSween Jr., A. Ghosh, R. E. Grimm, L. Wilson, E. D. Young, Thermal evolution models of asteroids, in *Asteroids III*, W. F. Bottke Jr., A. Cellino, P. Paolicchi, R. P. Binzel, Eds. (The University of Arizona Press, 2002), pp. 559–571.
53. C. M. O. Alexander, S. D. Newsome, M. L. Fogel, L. R. Nittler, H. Busemann, G. D. Cody, Deuterium enrichments in chondritic macromolecular material—Implications for the origin and evolution of organics, water and asteroids. *Geochim. Cosmochim. Acta* **74**, 4417–4437 (2010).
54. L. Piani, F. Robert, L. Remusat, Micron-scale D/H heterogeneity in chondrite matrices: A signature of the pristine solar system water? *Earth Planet. Sci. Lett.* **415**, 154–164 (2015).
55. B. Laurent, M. Roskosz, L. Remusat, F. Robert, H. Leroux, H. Vezin, C. Depecker, N. Nuns, J.-M. Lefebvre, The deuterium/hydrogen distribution in chondritic organic matter attests to early ionizing irradiation. *Nat. Commun.* **6**, 8567 (2015).
56. M. M. Grady, I. P. Wright, C. T. Pillinger, A preliminary investigation into the nature of carbonaceous material in ordinary chondrites. *Meteoritics* **24**, 147–154 (1989).
57. E. Deloule, F. Robert, J. C. Doukhan, Interstellar hydroxyl in meteoritic chondrules: Implications for the origin of water in the inner solar system. *Geochim. Cosmochim. Acta* **62**, 3367–3378 (1998).
58. C. M. O. Alexander, R. Bowden, M. L. Fogel, K. T. Howard, C. D. K. Herd, L. R. Nittler, The provenances of asteroids, and their contributions to the volatile inventories of the terrestrial planets. *Science* **337**, 721–723 (2012).
59. J. J. Barnes, D. A. Kring, R. Tartèse, I. A. Franchi, M. Anand, S. S. Russell, An asteroidal origin for water in the Moon. *Nat. Commun.* **7**, 11684 (2016).
60. J. F. Kerridge, Carbon, hydrogen and nitrogen in carbonaceous chondrites: Abundances and isotopic compositions in bulk samples. *Geochim. Cosmochim. Acta* **49**, 1707–1714 (1985).
61. F. Robert, The D/H ratio in chondrites. *Space Sci. Rev.* **106**, 87–101 (2003).
62. H. Balsiger, K. Altwegg, J. Geiss, D/H and $^{18}O/^{16}O$ ratio in the hydronium ion and in neutral water from in situ ion measurements in comet Halley. *J. Geophys. Res. A* **100**, 5827–5834 (1995).
63. P. Eberhardt, M. Reber, D. Krankowsky, R. R. Hodges, The D/H and $^{18}O/^{16}O$ ratios in water from comet P/Halley. *Astron. Astrophys.* **302**, 301 (1995).
64. D. Bockelée-Morvan, D. Gautier, D. C. Lis, K. Young, J. Keene, T. Phillips, T. Owen, J. Crovisier, P. F. Goldsmith, E. A. Bergin, D. Despois, A. Wootten, Deuterated water in comet C/1996 B2 (Hyakutake) and its implications for the origin of comets. *Icarus* **133**, 147–162 (1998).
65. R. Meier, T. C. Owen, H. E. Matthews, D. C. Jewitt, D. Bockelée-Morvan, N. Biver, J. Crovisier, D. Gautier, A determination of the HDO/H_2O ratio in comet C/1995 O1 (Hale-Bopp). *Science* **279**, 842–844 (1998).
66. D. Hutsemekers, J. Manfroid, E. Jehin, J.-M. Zucconi, C. Arpigny, The $^{16}OH/^{18}OH$ and OD/OH isotope ratios in comet C/2002 T7 (LINEAR). *Astron. Astrophys.* **490**, L31–L34 (2008).
67. G. L. Villanueva, M. J. Mumma, B. P. Bonev, M. A. DiSanti, E. L. Gibb, H. Böhnhardt, M. Lippi, A sensitive search for deuterated water in comet 8P/Tuttle. *Astrophys. J.* **690**, L5–L9 (2009).
68. P. Hartogh, D. C. Lis, D. Bockelee-Morvan, M. de Val-Borro, N. Biver, M. Küppers, M. Emprechtinger, E. A. Bergin, J. Crovisier, M. Renge, R. Moreno, S. Szutowicz, G. A. Blake, Ocean-like water in the Jupiter-family comet 103P/Hartley 2. *Nature* **478**, 218–220 (2011).
69. D. C. Lis, N. Biver, D. Bockelee-Morvan, P. Hartogh, E. A. Bergin, G. A. Blake, J. Crovisier, M. de Val-Borro, E. Jehin, M. Küppers, J. Manfroid, R. Moreno, M. Rengel, S. Szutowicz, A Herschel study of D/H in water in the Jupiter-family comet 45P/Honda-Mrkos-Pajdušáková and prospects for D/H measurements with CCAT. *Astrophys. J.* **774**, L3 (2013).
70. K. Altwegg, H. Balsiger, A. Bar-Nun, J. J. Berthelier, A. Bieler, P. Bochsler, C. Briois, U. Calmonte, M. Combi, J. De Keyser, P. Eberhardt, B. Fiethe, S. Fuselier, S. Gasc, T. I. Gombosi, K. C. Hansen, M. Hässig, A. Jäckel, E. Kopp, A. Korth, L. LeRoy, U. Mall, B. Marty, O. Mousis, E. Neefs, T. Owen, H. Rème, M. Rubin, T. Sémon, C.-Y. Tzou, H. Waite, P. Wurz, 67P/Churyumov-Gerasimenko, a Jupiter family comet with a high D/H ratio. *Science* **347**, 1261952 (2014).
71. J. P. Greenwood, S. Itoh, N. Sakamoto, P. Warren, L. Taylor, H. Yurimoto, Hydrogen isotope ratios in lunar rocks indicate delivery of cometary water to the Moon. *Nat. Geosci.* **4**, 79–82 (2011).
72. R. Tartèse, M. Anand, J. J. Barnes, N. A. Starkey, I. A. Franchi, Y. Sano, The abundance, distribution, and isotopic composition of hydrogen in the Moon as revealed by basaltic lunar samples: Implications for the volatile inventory of the Moon. *Geochim. Cosmochim. Acta* **122**, 58–74 (2013).
73. J. J. Barnes, I. A. Franchi, M. Anand, R. Tartèse, N. A. Starkey, M. Koike, Y. Sano, S. S. Russell, Accurate and precise measurements of the D/H ratio and hydroxyl content in lunar apatites using NanoSIMS. *Chem. Geol.* **337–338**, 48–55 (2013).
74. E. Füri, E. Deloule, A. Gurenko, B. Marty, New evidence for chondritic lunar water from combined D/H and noble gas analyses of single Apollo 17 volcanic glasses. *Icarus* **229**, 109–120 (2014).
75. R. Tartèse, M. Anand, F. M. McCubbin, S. M. Elardo, C. K. Shearer, I. A. Franchi, Apatites in lunar KREEP basalts: The missing link to understanding the H isotope systematics of the Moon. *Geology* **42**, 363–366 (2014).
76. E. Hauri, SIMS analysis of volatiles in silicate glasses, 2: Isotopes and abundances in Hawaiian melt inclusions. *Chem. Geol.* **183**, 115–141 (2002).
77. Q.-K. Xia, E. Deloule, Y.-B. Wu, D.-G. Chen, H. Cheng, Anomalously high δD values in the mantle. *Geophys. Res. Lett.* **29**, 4-1–4-4 (2002).
78. A. M. Shaw, E. H. Hauri, M. D. Behn, D. R. Hilton, C. G. Macpherson, J. M. Sinton, Long-term preservation of slab signatures in the mantle inferred from hydrogen isotopes. *Nat. Geosci.* **5**, 224–228 (2012).
79. M. Clog, C. Aubaud, P. Cartigny, L. Dosso, The hydrogen isotopic composition and water content of southern Pacific MORB: A reassessment of the D/H ratio of the depleted mantle reservoir. *Earth Planet. Sci. Lett.* **381**, 156–165 (2013).
80. L. L. Watson, I. D. Hutcheon, S. Epstein, E. Stolper, Water on Mars: Clues from deuterium/hydrogen and water contents of hydrous phases in SNC meteorites. *Science* **265**, 86–90 (1994).
81. L. A. Leshin, S. Epstein, E. M. Stolper, Hydrogen isotope geochemistry of SNC meteorites. *Geochim. Cosmochim. Acta* **60**, 2635–2650 (1996).
82. N. Z. Boctor, C. M. O. D. Alexander, J. Wang, E. Hauri, The sources of water in Martian meteorites: Clues from hydrogen isotopes. *Geochim. Cosmochim. Acta* **67**, 3971–3989 (2003).
83. J. P. Greenwood, S. Itoh, N. Sakamoto, E. Vicenzi, H. Yurimoto, Hydrogen isotope evidence for loss of water from Mars through time. *Geophys. Res. Lett.* **35**, L05203 (2008).
84. L. J. Hallis, G. J. Taylor, K. Nagashima, G. R. Huss, Magmatic water in the martian meteorite Nakhla. *Earth Planet. Sci. Lett.* **359–360**, 84–92 (2012).
85. T. Usui, C. M. O. D. Alexander, J. Wang, J. I. Simon, J. H. Jones, Origin of water and mantle-crust interactions on Mars inferred from hydrogen isotopes and volatile element abundances of olivine-hosted melt inclusions of primitive shergottites. *Earth Planet. Sci. Lett.* **357–358**, 119–129 (2012).
86. S. Hu, Y. Lin, J. Zhang, J. Hao, L. Feng, L. Xu, W. Yang, J. Yang, NanoSIMS analyses of apatite and melt inclusions in the GRV 020090 Martian meteorite: Hydrogen isotope evidence for recent past underground hydrothermal activity on Mars. *Geochim. Cosmochim. Acta* **140**, 321–333 (2014).
87. T. Usui, C. M. O. D. Alexander, J. Wang, J. I. Simon, J. H. Jones, Meteoritic evidence for a previously unrecognized hydrogen reservoir on Mars. *Earth Planet. Sci. Lett.* **410**, 140–151 (2015).
88. P. Mane, R. Hervig, M. Wadhwa, L. A. J. Garvie, J. B. Balta, H. Y. McSween Jr., Hydrogen isotopic composition of the Martian mantle inferred from the newest Martian meteorite fall, Tissint. *Meteorit. Planet. Sci.* **51**, 2073–2091 (2016).
89. J. Geiss, G. Gloeckler, Abundances of deuterium and helium-3 in the protosolar cloud. *Space Sci. Rev.* **84**, 239–250 (1998).
90. E. Lellouch, B. Bézard, T. Fouchet, H. Feuchtgruber, T. Encrenaz, T. de Graauw, The deuterium abundance in Jupiter and Saturn from ISO-SWS observations. *Astron. Astrophys.* **670**, 610–622 (2001).
91. H. Feuchtgruber, E. Lellouch, B. Bézard, Th. Encrenaz, Th. de Graauw, G. R. Davis, Detection of HD in the atmospheres of Uranus and Neptune: A new determination of the D/H ratio. *Astron. Astrophys.* **341**, L17–L21 (1999).
92. T. M. Donahue, J. H. Hoffman, R. R. Hodges Jr., A. J. Watson, Venus was wet: A measurement of the ratio of deuterium to hydrogen. *Science* **216**, 630–633 (1982).
93. H. Skogby, D. R. Bell, G. R. Rossman, Hydroxide in pyroxene: Variations in the natural environment. *Am. Mineral.* **75**, 764–774 (1990).
94. D. R. Bell, G. R. Rossman, Water in Earth's mantle: The role of nominally anhydrous minerals. *Science* **255**, 1391–1397 (1992).

95. D. R. Bell, G. R. Rossman, R. O. Moore, Abundance and partitioning of OH in a high-pressure magmatic system: Megacrysts from the Monastery kimberlite, South Africa. *J. Petrol.* **45**, 1539–1564 (2004).
96. A. H. Peslier, A review of water contents of nominally anhydrous natural minerals in the mantles of Earth, Mars and the Moon. *J. Volcanol. Geotherm. Res.* **197**, 239–258 (2010).
97. R. Sundvall, R. Stalder, Water in upper mantle pyroxene megacrysts and xenocrysts: A survey study. *Am. Mineral.* **96**, 1215–1227 (2011).
98. A. R. Sarafian, S. G. Nielsen, H. R. Marschall, G. A. Gaetani, E. H. Hauri, K. Righter, E. Sarafian, Angrite meteorites record the onset and flux of water to the inner solar system. *Geochim. Cosmochim. Acta* **212**, 156–166 (2017).

Acknowledgments: We are grateful to R. Hervig and Z. Peeters for assistance with the IMS 6f and NanoSIMS measurements. We thank JAXA curatorial facility for providing Itokawa particles, and the Smithsonian Institution and K. M. Kumamoto at Stanford University for the reference samples. M.B. would like to thank R. Jansen and S. Desch for fruitful discussions. **Funding:** M.B. was funded by her startup funds from Arizona State University. **Author contributions:** M.B. designed and supervised the project. Z.J. prepared samples and collected and processed data. Z.J. and M.B. wrote the manuscript. **Competing interests:** The authors declare that they have no competing interests. **Data and materials availability:** All data needed to evaluate the conclusions in the paper are present in the paper and/or the Supplementary Materials. Additional data related to this paper may be requested from the authors.

Submitted 22 October 2018
Accepted 15 March 2019
Published 1 May 2019
10.1126/sciadv.aav8106

Citation: Z. Jin, M. Bose, New clues to ancient water on Itokawa. *Sci. Adv.* **5**, eaav8106 (2019).

New clues to ancient water on Itokawa

Ziliang Jin and Maitrayee Bose

Sci Adv **5** (5), eaav8106.
DOI: 10.1126/sciadv.aav8106